Book of Tutorials and Abstracts

European
Microbeam Analysis Society

University of BRISTOL

Mineralogical Society

EMAS 2018

13th EMAS Regional Workshop

MICROBEAM ANALYSIS IN THE EARTH SCIENCES

4 - 7 September 2018

University of Bristol, Wills Hall, Bristol, Great Britain

Organised in collaboration with:
Mineralogical Society of Great Britain and Ireland
and
University of Bristol

ANALYSING SILICATE MELT INCLUSIONS

E.C. Hughes[1], B. Buse[1], S.L Kearns[1], G. Kilgour[2], H. Mader[1] and J. Blundy[1]

1 University of Bristol, School of Earth Sciences
Wills Memorial Building, Queens Road, Bristol BS8 1RJ, Great Britain
2 Wairakei Research Centre, GNS Science
114 Karetoto Road, RD4, 3384 Taupo, New Zealand
e-mail: ery.hughes@bristol.ac.uk

ABSTRACT

Melt inclusion (MI) chemistry can be used to reconstruct the history of magmas prior to eruption, such as tracking changes in melt composition, volatile contents, and oxygen fugacity (fO_2). MIs are small (10s - 100s μm in diameter) and require microanalytical techniques for their analysis. Here, we cover how to use electron probe microanalysis (EPMA) to measure major and minor element chemistry, volatile concentrations (directly and by difference), and Fe oxidation state, at the high spatial resolution needed for MIs. MIs are glasses, which are insulators, hence sub-surface charging occurs during analysis which can alter the glass composition and X-ray intensities during analysis, which must be considered to ensure accurate and precise data.

1. INTRODUCTION

Melt inclusions (MIs) are small pockets of melt trapped inside crystals as they grow from magmas, which quench to glass upon eruption (Fig. 1). They sample the melt as it ascends to the surface, providing a unique insight into changes to melt composition prior to eruption. Changes in major and minor element chemistry can be used to investigate crystallisation histories and magma mixing [1]. Volatile (H_2O, CO_2, S, Cl, etc.) concentrations can be used to estimate magma volatile budgets, degassing pathways, and entrapment pressures which can be used to investigate the architecture of magma plumbing systems [2]. As Fe and S can have multiple valences, their oxidation state in melts can be used to estimate the oxygen fugacity (fO_2) [3].

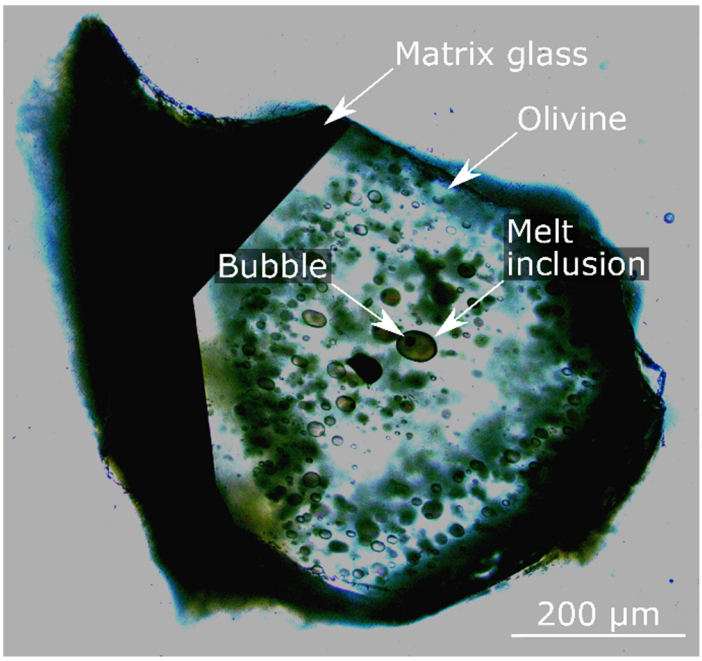

Figure 1. Reflected-light image of multiple MI suites in an olivine crystal from Stromboli, Italy. Olivine host, surrounding matrix glass, melt inclusion, and a bubble within the melt inclusion are labelled.

The composition and phases present in MIs can be modified post-entrapment, therefore care must be taken when collecting and interpreting MI data. The host can crystallise on the inclusion walls (Post-Entrapment Crystallisation, PEC), changing the MI composition but this can be corrected for after analysis [4]. Bubbles can form within the MI, due to differential contraction of the host and glass, which forms a void into which volatiles (especially CO_2) can diffuse into, thus lowering their concentration in the melt [5] (Fig. 1). The CO_2 content of the bubble can be measured using Raman and added back into the melt if needed. At elevated temperatures (e.g., lava flows), H can diffuse out of (or into) the MI whilst trying to equilibrate with the surrounding magma, which changes the H_2O concentration in the MI [6]. This can also lead to changes in Fe and S oxidation state, which can affect estimations of fO_2 and reduce the S concentration if S precipitates out of the melt [6].

Due to their size, MIs require microanalytical techniques to analyse them. Volatiles (H_2O, and sometimes CO_2) can be analysed using SIMS, FTIR, and Raman; trace elements using LA-ICP-MS; and Fe oxidation state using μXANES, synchrotron Mössbauer, and Raman. SIMS and LA-ICP-MS require the MI so be exposed with a flat, polished surface, whilst μXANES, synchrotron Mössbauer, and FTIR require the MI to be intersected at both the top and bottom surfaces as they are transmission techniques. Raman can analyse unexposed MIs if the host is transparent.

The electron probe is commonly used to analyse silicate glasses because it can measure a wide range of elements accurately and precisely at high spatial resolution. Analysis times are short (minutes), the equipment is widely available, sample preparation is simple (single, flat polished surface). It can also be used to measure the volatile content (H_2O+CO_2) by difference and oxidation states of Fe and S. Glasses are insulators and therefore require a conductive coat (e.g., C or Au) for electron probe microanalysis (EPMA), otherwise charge builds up on the surface preventing analysis. However, this conductive coat does not prevent some of the incident electrons being trapped within sample, generating an internal electric field [7]. This electric field can modify the glass composition by causing mobile ions to migrate in response to the negative charge at depth. For instance Na^+ can migrate towards the build-up of charge, and Fe and S can oxidise in response to H^+ or alkali migration [8-10]. Additionally, the electric field can modify the generation and emittance of X-rays as the incident electrons are decelerated within the sample due to the electric field [7]. This results in fewer X-rays being generated, but these X-rays are generated shallower in the sample and hence less likely to be absorbed. This results in higher X-ray intensity for soft X-rays (e.g., O-Kα) but lower X-ray intensity for hard X-rays (e.g., Fe-Kα) [7]. Changes in X-ray intensities and sample composition during EPMA need to be accounted for when analysing glasses to obtain precise and accurate analyses.

2. *VOLATILES BY DIFFERENCE*

The electron probe can measure the major and minor element chemistry, including volatiles such as S and Cl, directly, and the volatile content ($H_2O + CO_2$) indirectly using volatiles by difference (VBD) [1, 8, 11-13]. Hydrogen cannot be measured directly using the electron probe and the CO_2 content of melts tends to be below detectability (10s - 1000s ppm CO_2). VBD is calculated by measuring all the other elements in the glass, converting them to oxides (if O is not measured), and then the difference between the analytical total and 100 wt% is the unmeasured volatile content. The oxidation state of Fe, and S if sufficiently high in concentration, must be known for basalts and pantellerites when O is not measured to convert them to oxides.

As a by difference technique, care must be taken to analyse all the other elements precisely to achieve small errors on VBD, as the error is the quadratic sum of all the element errors. Typically, analyses are carried out with a 15 - 20 kV accelerating voltage. Beam currents are chosen to achieve the precision required in a reasonable time-frame (e.g., 2 - 10 nA) and to minimise beam damage, and beam diameters depend on the size of the MIs (e.g., 4 - 15 μm). Hydrogen must be specified as an element in the matrix correction because otherwise the mean atomic number (MAN) of the sample will be incorrectly calculated. This is important for determining the amount of backscattering and the depth distribution of X-rays, and including the absorption of X-rays due to the O within H_2O [14]. If H_2O is not included in the matrix correction, VBD can be overestimated by ~ 1 wt% [15]. An example set-up for VBD for basaltic glasses is shown in Table 1. The peak positions of some X-ray lines are oxidation state (e.g., S-Kα [17]) dependent, therefore similar standards to the unknowns should be used for peaking up where possible to avoid underestimating concentrations due to being off peak. As melt inclusions are surrounded by a mineral-host, secondary fluorescence might elevate the apparent concentration of traces in the glass that are present at high concentrations in the host mineral (e.g., Ca in rhyolitic MIs hosted in plagioclase), but this can be corrected for [18].

Sub-surface charging has two effects on the analysis of glasses. Firstly, the generated electric field causes mobile elements (e.g., Na and K) to migrate towards the build-up of charge at depth [8], causing their X-ray intensities to reduce over time. Concurrently, the X-ray intensity of immobile elements (e.g., Si and Al), increases over time due to "grow-in" as their relative concentration increases [19]. This is more likely to happen in hydrous or alkali-rich glasses, and high-silica glasses [8, 10, 20]. This can be mitigated by either using low beam currents and/or large beam diameters [21], but this either reduces precision, increases analytical times, or reduces spatial resolution. Also, there is a ca. 20 μm diameter limit on the maximum beam size as beyond this wavelength-dispersive X-ray spectrometers (WDS) go out of focus. Alternatively, the X-ray intensity can be monitored over time (time-dependent intensity (TDI) measurements, [22]) and extrapolated to time zero to measure the initial concentration of these elements (Fig. 2a). As these changes are not always linear, only elements measured at the beginning of an analysis can be corrected in this way. MAN backgrounds can be used instead of off-peak backgrounds, reducing

Table 1. Example set-up for VBD analysis of basaltic glasses: 15 kV accelerating voltage, 10 nA beam current, and 5 - 10 µm beam diameter.

Spectrometer – Crystal				
1 – PETJ	2 – TAP	3 – TAPH	4 – PETH	5 – LIFL
Ca*	Si*	Na*	K*	Fe*
Wollastonite	*Albite*	*Albite*	*Sanidine*	*Andradite*
Ti	Al	Mg	P	Mn
TiO_2	*Sanidine*	*SJIO*	*Durango apatite*	*Mn metal*
Cl			S	
NaCl			*VG2*	
			Barite	

Notes: Elements listed in order of analysis and were peaked on the 1st standard in *italics* and calibrated on the 2nd standard if different. VG2 is a Smithsonian Microbeam basaltic glass standard and SJIO is St John's Island Olivine. Peak counting times are 60 s, except K which are 120 s. MAN backgrounds were used. * indicates TDI measurements collected.

analysis time by approximately half and therefore beam damage as well. MAN backgrounds use the measured relationship between background counts and MAN to calculate the background intensity (Fig. 2b) [23].

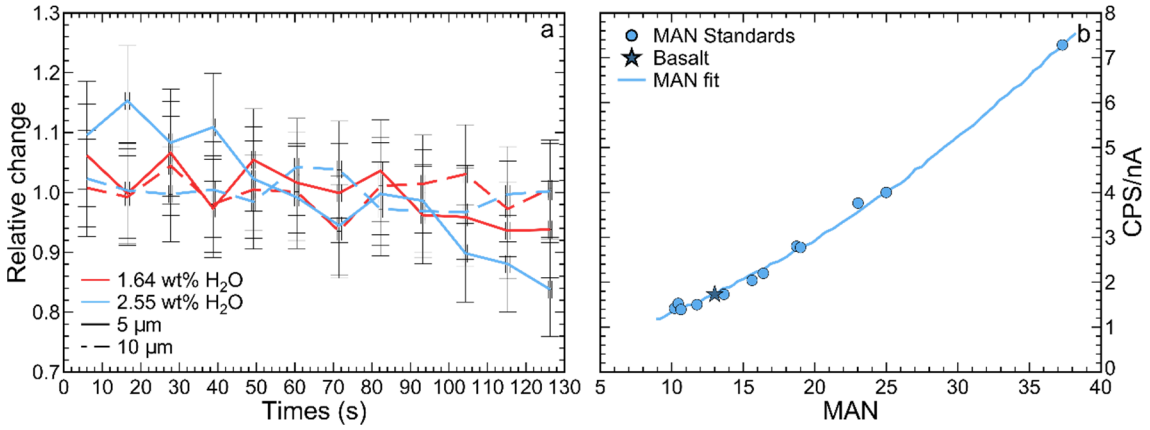

Figure 2. Example for Na of (a) TDI data for two basaltic glasses with different H_2O contents (MAS.1.B9 = 1.64 wt%, and MAS.1.B4 = 2.55 wt% from [24]) at 5 and 10 µm beam diameters; and (b) MAN background calibration with the MAN standards and fit, with the star showing the MAN for basaltic glass (BCR-2).

Secondly, the generated electric field reduces the intensity of the emitted X-rays because the electrons decelerate when they enter the sample due to the negative charge at depth [7]. The reduction in intensity is related to the maximum electric field strength in the sample, which is a function of the density of trapped charge. If the standards and unknowns trap different quantities

of charge, for instance as glasses trap more electrons than minerals because there are more charge trapping sites, [7], the concentration will be underestimated. This results in an underestimation in the analytical total and hence an overestimation of VBD, which can be seen in literature and modelled data using the Monte Carlo programme *Win X-ray* [25] (Fig. 3a). In practice, the underestimation of any individual element is small and typically within analytical error, hence only VBD itself needs to be corrected. This can be done by calibrating VBD using a set of hydrous glass standards with known volatile content (H_2O and ideally CO_2) and Fe oxidation state, at the same analytical conditions and during the same session (Fig. 3b). This improves the accuracy of VBD to within 0.1 wt% from an offset of the order +1 wt%.

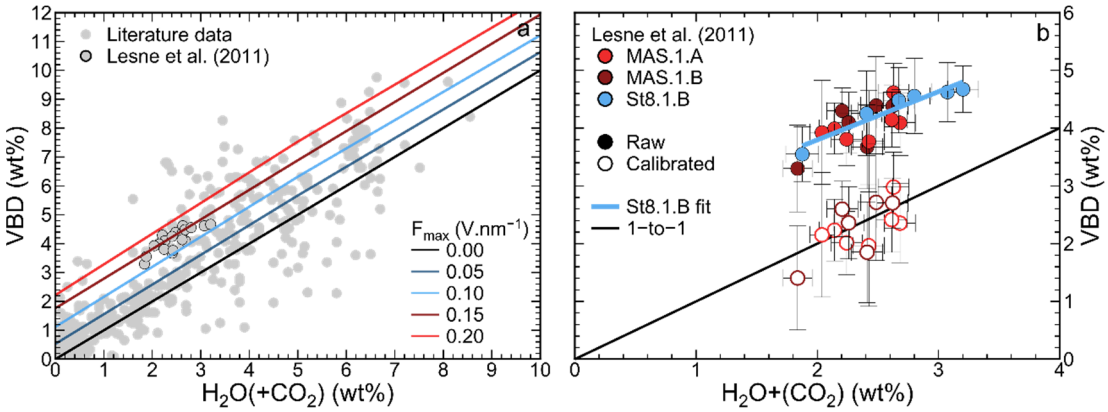

Figure 3. VBD (including Fe oxidation state data if available) against volatile content (H_2O, and CO_2 where available): (a) literature data (n = 525) and modelled VBD using *Win X-ray* [25]; and (b) raw and calibrated VBD using data from [24].

3. *IRON OXIDATION STATE*

The Fe oxidation state (Fe^{2+}/Fe_T) can be measured using the electron probe by analysing the Fe-Lα and Fe-Lβ lines, which change peak position and height depending on the concentration, oxidation state and coordination of Fe [26] (Fig. 4). The peak shift method uses the peak position of the Fe-Lα line in combination with the total Fe content (Fe_T) to measure Fe^{2+}/Fe_T [27, 28] (Fig. 4). The flank method uses the ratio of the intensities on the high wavelength flank of Fe-Lβ (Fe-Lβ$_f$) to the low wavelength flank of Fe-Lα (Fe-Lα$_f$) (Fe-Lβ$_f$/Fe-Lα$_f$) to calculate Fe^{2+} content, which can be converted to Fe^{2+}/Fe_T by measuring Fe_T [29, 30] (Fig. 4). The flank positions are very sensitive to changes in Fe^{2+}/Fe_T, hence the flank method is more sensitive than the peak shift method. Both methods have been successfully applied to silicate glasses [20, 28], but sub-surface charging causes changes in the Fe oxidation state during analysis. The stage can be moved during analysis to reduce the dose per unit area and minimise these effect, but it is not possible to move the stage when analysing MIs due to their small size. Instead, a combination of TDI measurements and the flank method (TDR flank method) can be used to obtain high spatial resolution (20 - 60 µm in diameter) analysis of Fe^{2+}/Fe_T within ±0.1 [10]. The change in Fe oxidation state is monitored by measuring Fe-Lβ$_f$/Fe-Lα$_f$ over time, and then corrected to time zero to calculate Fe^{2+}/Fe_T.

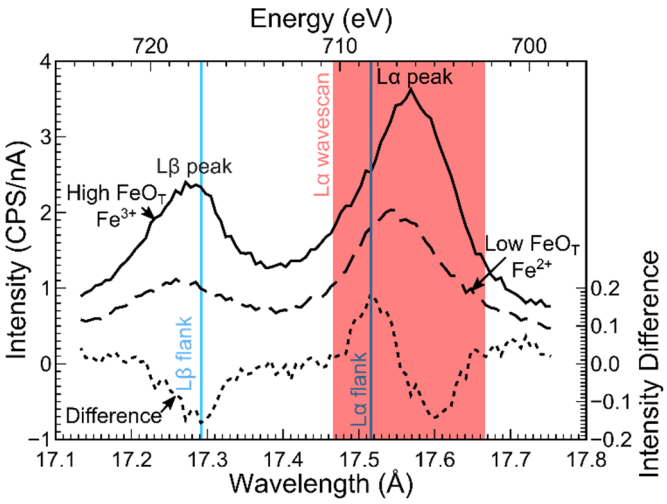

Figure 4. Example wavescans of a high FeO_T, oxidised and low FeO_T, reduced glass. Difference curve is calculated once the wavescans have been normalised to their Fe-Lα peak intensity. Red box indicates wavelengths analysed for the Peak Shift Method, and blue lines indicate wavelengths analysed for the flank method. Modified from [10].

Flank positions can be identified by collecting wavescans of two glasses with different Fe^{2+}/Fe_T and Fe_T, ideally as extreme as possible [30]. An example set-up is shown in Table 2, but critically the stage must be moved (1 μs^{-1}) whilst collecting the wavescans to avoid beam damage. To improve the signal to noise ratio, wavescans can be combined from many TAP-type crystals (e.g., TAP, TAPH, and LTAP), and multiple wavescans can be collected on each crystal. The wavescans are then normalised to the maximum intensity of their Fe-Lα peak, and the difference between them is calculated (Fig. 4). The Fe-Lα_f is the maximum and the Fe-Lβ_f is the minimum of the difference curve. To avoid collecting wavescans for every analytical session (which wastes time and standard material), it is best to measure the flank position on each crystal relative to a different peak, easily analysed peak on the same crystal, such as F-Kα on MgF_2 or 9th order Fe-Kα on Fe-metal.

Table 2. Example set-up for identifying flank positions.

Analytical conditions	Accelerating voltage 15 kV	Beam current 50 nA	Beam diameter 10 µm
Wavescan set-up	No. steps 100	Step size (L) 0.071 mm	Dwell time 0.5 s
Crystals	TAP	TAP	TAPH

Note: Stage must be moving (1 μs^{-1}) during analysis; step size (L) is for JEOL instruments; and the accelerating voltage must be the same as those used for analysis.

An example set-up for TDR flank method measurements are shown in Table 3. As many TAP-type crystals (e.g., TAP, TAPH, LTAP) can be used to improve the counting statistics. For the set-up in Table 3, the TAPH crystal had twice as many counts as the TAP crystals, and the Fe-Lβ peak is roughly half the intensity of the Fe-Lα peak, hence two TAP crystals were used to analyse Fe-Lα_f and the TAPH for Fe-Lβ_f. Other crystal combinations will work provided the same set-up is used on the standards and unknowns. Fe-Kα and K-Kα are additionally analysed to check for sample homogeneity and monitor beam damage. Spectrometers with TAP-type crystals are initially peaked up on the X-ray line the flank positions have been measured relative to. Differential mode is used to remove the interference of the 9th order Fe-Kα and PHA windows are set using F-Kα on MgF_2. The peak positions are then changed to the correct flank position.

Table 3. Example set-up for TDR flank method measurements.

Analytical conditions	Accelerating voltage 15 kV		Beam current 50 nA		Beam diameter 4 – 15 μm	
Instrument set-up	Crystal X-ray line	TAP Fe*L*α$_f$	TAP Fe*L*α$_f$	TAPH Fe*L*β$_f$	LLIF Fe*K*α	PETH K*K*α
Count times	No. intervals 24		Interval time 5 s		Total time ~150 s	

Notes: Beam diameter depends on glass composition being analysed (use a larger beam for more unstable glasses); and BCR-2 is the USGS basaltic glass standard Columbia River Basalt 2.

TDI measurements are collected on the same analysis spot (e.g., 24 intervals of 5 s each) and ten repeat analyses are collected per sample. The beam diameter should be appropriate for the MIs being analysed (e.g., 4 μm diameter beam × 10 analyses ≈ 20 μm diameter MI), but also large enough that the change in Fe oxidation state is not too quick to be observed. Reduced glasses oxidise, whereas oxidised glasses reduce during analysis even if they are anhydrous. Generally, hydrous glasses are more unstable than anhydrous glasses, as H^+ migration causes oxidation, and high-silica glasses (with sufficient Fe) are more unstable than low-silica glasses. For anhydrous to hydrous basaltic glasses, a 4 μm beam diameter produces good results, whereas for anhydrous to hydrous peralkaline glasses a 15 μm beam diameter is required. Hughes *et al.* [10] has further details on the compositional controls on glass stability.

Standards and unknowns should be collected in the same analytical session using the same accelerating voltage. To process the data, check for sample homogeneity using the Fe-Kα and K-Kα counts: remove outliers and if the sample is heterogenous discard it. Fe-Lβ_f/Fe-Lα_f is the combined (if more than one TAP-type crystal was used) counts for Fe-Lβ_f divided by the combined counts for Fe-Lα_f. An exponential function is fitted to the Fe-Lβ_f/Fe-Lα_f data of the form:

$$I_t = (I_0 - I_\infty)\exp[(I'_0 t)/(I_0 - I_\infty)] + I_\infty$$

where I is Fe-Lβf/Fe-Lαf and the subscript refers to the time t. If this fails to converge, I_∞ is set to the last measured value of Fe-Lβf/Fe-Lαf. If it still fails to converge, I is constant with time (i.e., the sample is stable) and the average of Fe-Lβf/Fe-Lαf is used. An R-code for processing is available in [10].

A calibration curve of I_0 (i.e., initial Fe-Lβf/Fe-Lαf) against Fe^{2+} concentration of standards is used to calculate the Fe^{2+} content of the unknown glasses (Fig. 5a). Basaltic glasses require a different calibration curve to peralkaline glasses. To convert to Fe^{2+}/Fe_T, Fe_T must be also measured, for instance using standard EPMA (e.g., Table 1). The technique has been tested on hydrous (0 - 4 wt% H_2O) silicate glasses with low-silica (43 - 56 wt% SiO_2) and peralkaline (70 – 76 wt% SiO_2) compositions with $FeO_T > 5$ wt% (below this there is insufficient Fe to obtain reliable results), and a precision of ±0.1 Fe^{2+}/Fe_T was obtained (Fig. 5b). Fe oxidation state can be converted to fO_2 if the pressure, temperature and glass composition are known, for instance using [3].

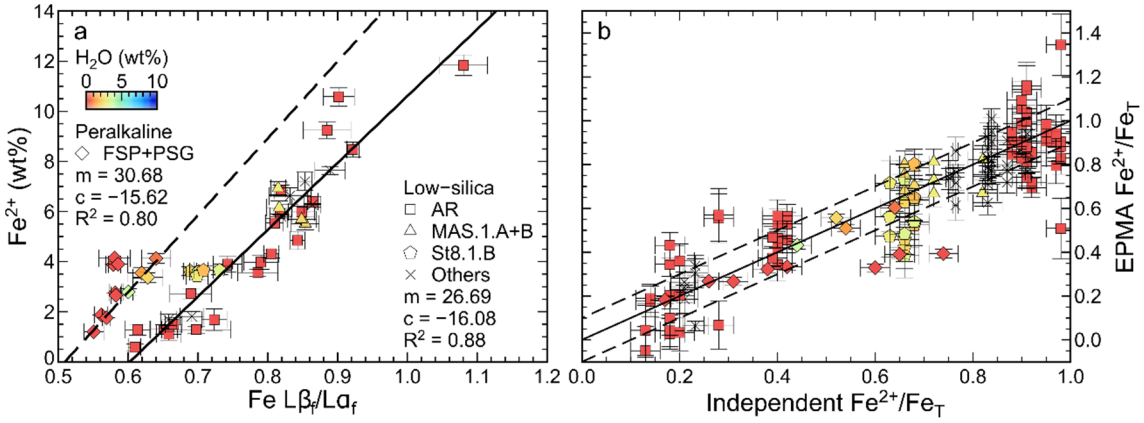

Figure 5. (a) Example calibration curve of independently constrained Fe^{2+} against corrected Fe-Lβf/Fe-Lαf for low-silica and peralkaline glasses; and (b) EPMA against independently constrained Fe^{2+}/Fe_T for the same glasses. Symbol shape indicates glass composition, and colour indicates H_2O content. Figure modified from [10].

4. *CONCLUSIONS*

The electron probe can be used to measure the major and minor element chemistry (one standard deviation, 1σ, ±1 % relative), volatile (1σ ±0.6 wt%), and Fe oxidation state (1σ ±0.1) of MIs. As MIs are made of glass which is an insulator, all EPMA is affected by sub-surface charging which modifies the emitted X-ray intensities and glass composition, potentially leading to spurious results. To obtain accurate and precise data, TDI data should be collected when the glass composition changes (e.g., Na loss, Si "grow-in", and Fe oxidation and reduction), and VBD should be calibrated to correct for X-ray intensity reduction.

5. ACKNOWLEDGEMENTS

ECH is supported by a NERC GW4+ DTP studentship from the Natural Environment Research Council (NE/L002434/1) and is thankful for the support and additional funding from CASE partner GNS Science, New Zealand.

6. REFERENCES

[1] Blundy J D and Cashman K V 2008 *Rev. Mineral. Geochem.* **69** 179-240
[2] Métrich N and Wallace P J 2008 *Rev. Mineral. Geochem.* **69** 363-402
[3] Kress V C and Carmichael I S E 1991 *Contrib. Mineral. Petrology* **108** 82-92
[4] Danyushevsky L V and Plechov P 2011 *Geochem. Geophys. Geosystems* **12** Q07021
[5] Wallace P J, *et al.* 2015 *Am. Mineralogist* **100** 787-794
[6] Hartley M E, *et al.* 2017 *Earth Planet. Sci. Lett.* **479** 192-205
[7] Cazaux J 1996 *X-ray Spectrom.* **25** 265-280
[8] Humphreys M C S, *et al.* 2006 *Am. Mineralogist* **91** 667-679
[9] Jbara O, *et al.* 1995 *J. Appl. Phys.* **78** 868-875
[10] Hughes E C, *et al.* 2018 *Am. Mineralogist* (accepted)
[11] Devine J D, *et al.* 1995 *Am. Mineralogist* **80** 319-328
[12] King P L, *et al.* 2002 *Am. Mineralogist* **87** 1077-1089
[13] Nash W P 1992 *Am. Mineralogist* **77** 453-457
[14] Donovan J J and Vicenzi E P 2008 *Microsc. Microanal.* **14** 1274-1275
[15] Roman D C, *et al.* 2006 *Bull. Volcanol.* **68** 240-254
[16] White E W and Gibbs G V 1967 *Am. Mineralogist* **52** 985-993
[17] Faessler A and Goehring M 1952 *Naturwissenschaften* **39** 169-177
[18] Llovet X and Galan G 2003 *Am. Mineralogist* **88** 121-130
[19] Morgan G B and London D 2005 *Am. Mineralogist* **90** 1131-1138
[20] Zhang C, *et al.* 2018 *Am. Mineralogist* (accepted)
[21] Hayward C 2011 *The Holocene* **22** 119-125
[22] Nielsen C H and Sigurdsson H 1981 *Am. Mineralogist* **66** 547-552
[23] Donovan J J and Tingle T N 1996 *Microsc. Microanal.* **2** 1-7
[24] Lesne P, *et al.* 2011 *J. Petrology* **52** 1737-1762
[25] Demers H and Gauvin R 2004 *Microsc. Microanal.* **10** 776-782
[26] Gopon P, *et al.* 2013 *Microsc. Microanal.* **19** 1698-1708
[27] Fialin M, *et al.* 2001 *Am. Mineralogist* **86** 456-465
[28] Fialin M, *et al.* 2004 *Am. Mineralogist* **89** 654-662
[29] Hofer H E, *et al.* 1994 *Eur. J. Mineralogy* **6** 407-418
[30] Hofer H E and Brey G P 2007 *Am. Mineralogist* **92** 873-885